Report

Cell PRESS

Proteoglycan-Mediated Axon Degeneration Corrects Pretarget Topographic Sorting Errors

Fabienne E. Poulain[1,]* and Chi-Bin Chien[1,2]
[1]University of Utah, Neurobiology and Anatomy Department, Salt Lake City, UT 84132, USA
[2]This author is deceased
*Correspondence: fpoulain@genetics.utah.edu
http://dx.doi.org/10.1016/j.neuron.2013.02.005

SUMMARY

Proper arrangement of axonal projections into topographic maps is crucial for brain function, especially in sensory systems. An important mechanism for map formation is pretarget axon sorting, in which topographic ordering of axons appears in tracts before axons reach their target, but this process remains poorly understood. Here, we show that selective axon degeneration is used as a correction mechanism to eliminate missorted axons in the optic tract during retinotectal development in zebrafish. Retinal axons are not precisely ordered during initial pathfinding but become corrected later, with missorted axons selectively fragmenting and degenerating. We further show that heparan sulfate is required non-cell-autonomously to correct missorted axons and that restoring its synthesis at late stages in a deficient mutant is sufficient to restore topographic sorting. These findings uncover a function for developmental axon degeneration in ordering axonal projections and identify heparan sulfate as a key regulator of that process.

INTRODUCTION

Organization of neuronal connections into topographic maps is crucial for processing information. One widely accepted mechanism that determines the topographic order of axon terminals relies on specific axon-target interactions, in which axons with a unique profile of receptors interpret guidance cues distributed in a gradient within the target (Feldheim and O'Leary, 2010). Another mechanism far less well understood but also contributing to map formation is pretarget topographic sorting of axons along tracts. In many systems, axons are preordered en route to their target according to their identity and/or positional origin. For instance, olfactory sensory neurons expressing specific odorant receptors and projecting to different locations in the olfactory bulb are presorted in the axon bundle (Bozza et al., 2009; Imai et al., 2009; Satoda et al., 1995). Similarly in the visual system, retinal axons are preordered along the dorsoventral axis in the optic tract before reaching the optic tectum (or superior colliculus in mammals) (Plas et al., 2005; Scholes, 1979). This specific ordering of axons is well conserved among vertebrates and probably involves local regulatory mechanisms independent

from brain targets, since sorting of retinal and olfactory axons is preserved in the complete absence of tectum or olfactory bulb, respectively (Imai et al., 2009; Reh et al., 1983; St John et al., 2003).

While it appears to have an instructive role in map formation (Imai et al., 2009), how pretarget axon sorting is established and regulated during development is poorly understood. Some signals have been implicated in organizing axons along tracts (Imai et al., 2009; Plas et al., 2008), but the cellular mechanisms by which axons are precisely ordered have never been described. Do axons segregate during initial growth cone guidance, or are their trajectories refined at later stages? If axonal projections are corrected, what are the cellular and molecular mechanisms involved? Exploring these questions requires the ability to directly visualize growing axons in live embryos, an approach that can be challenging in mammalian models. We took advantage of the unique accessibility and transparency of the zebrafish embryo to monitor pretarget sorting of retinal axons in vivo as they elongate along the optic tract. In all vertebrates, axons originating from the dorsal and ventral retina are topographically reorganized after crossing the chiasm so that dorsal and ventral axons segregate respectively into the ventral and dorsal branches of the optic tract (Chan and Guillery, 1994; Plas et al., 2005; Scholes, 1979). Here we report that some dorsal axons misroute along the dorsal branch as they first elongate along the tract, indicating that sorting is not precisely established by initial growth cone guidance. Instead, topographic order is achieved through the selective degeneration of missorted dorsal axon trajectories. In contrast to correctly sorted axons, missorted dorsal axons stop their elongation before reaching the tectum and rapidly fragment all along their length. We further demonstrate that this specific degeneration does not require neuronal activity of retinal ganglion cells (RGCs) or the activation of p53-dependent apoptotic pathways. It depends, however, on the presence of heparan sulfate (HS), which acts non-cell-autonomously for correcting missorted axons and establishing pretarget topographic sorting. Thus, our study not only reveals a function for developmental axon degeneration in ordering axonal projections, but also identifies HS as a key regulator required for topographic sorting error correction.

RESULTS

Sorting of Retinal Axons Is Achieved through a Correction Mechanism

To determine whether dorsal and ventral axons are first sorted during initial growth cone guidance along the tract, we
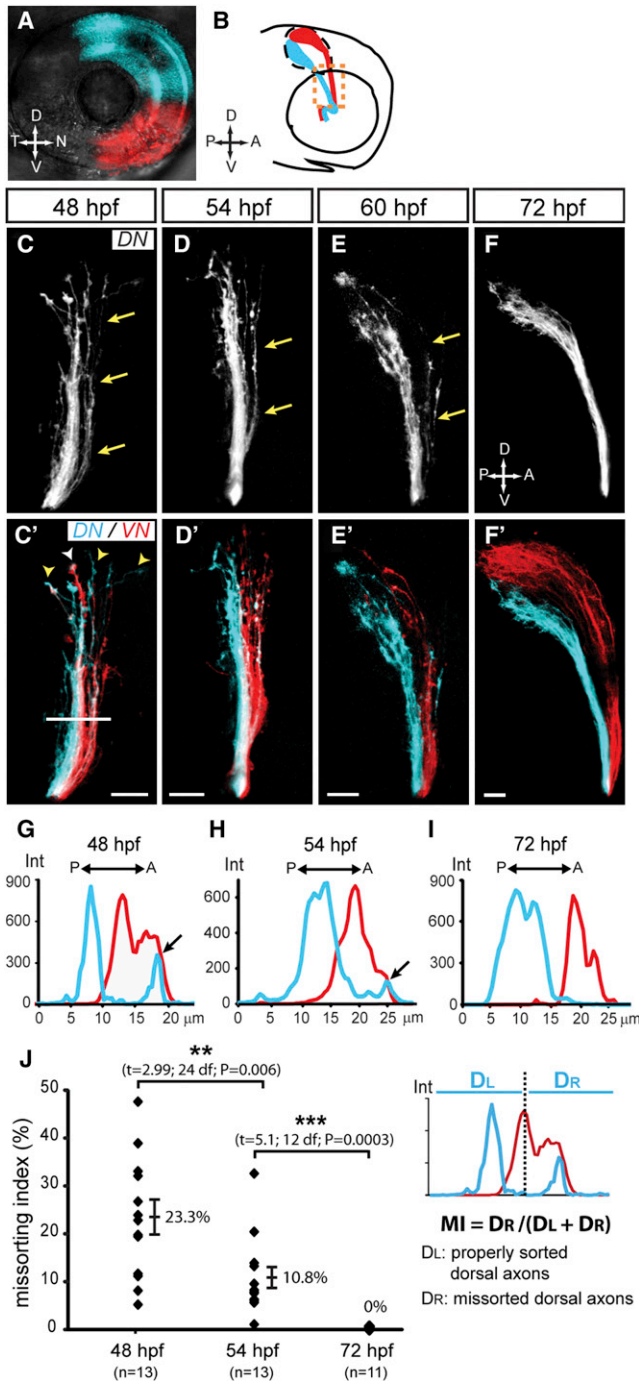
CrossMark

performed precise topographic dye labeling of the dorsonasal (DN) and ventronasal (VN) quadrants of the retina in zebrafish embryos fixed at early stages (Figure 1A). Corresponding DN and VN axonal projections were visualized along the optic tract after removing the contralateral eye (Figure 1B). At 48 hr postfertilization (hpf), when the first axons elongate along the tract and reach the tectum (Burrill and Easter, 1995; Stuermer, 1988), DN and VN axons were not precisely sorted. Some DN axons elongated along with VN axons in the most dorsal (anterior) part of the tract (Figures 1C and 1C′, see Figures S1A and S1A′ available online). Moreover, growth cones were intermingled and did not segregate along distinct paths according to their dorsoventral identity (Figure 1C′). At 54 and 60 hpf, sorting was more apparent, but some DN axons were still visible in the dorsal part of the tract, growing along or sometimes dorsally to VN axons (Figures 1D–1E′, Figures S1B and S1C′). In contrast, at 72 hpf, when projections are more mature, DN and VN axons were completely segregated (Figures 1F and 1F′). We analyzed and quantified the distribution and levels of DN and VN signals across the optic tract (Figures 1G–1I) and generated a missorting index (MI) measuring the proportion of missorted DN axons (Figure 1J). While sorting of VN axons was accurate at all stages observed, a significant number of DN axons were clearly missorted at 48 hpf (MI 23.3%). Missorting of DN axons progressively decreased at later stages (MI 10.8% at 54 hpf) and was no longer observed at 72 hpf. These results indicate that pretarget sorting of retinal axons is not precisely established during initial growth cone guidance along the optic tract but rather is achieved by correcting missorted DN projections.

Missorted DN Axons Undergo Selective Developmental Degeneration

How are missorted DN axons corrected? Missorted axons could respond to a specific cue and retract, as has been shown during pathfinding error correction at the chiasm (Hutson and Chien, 2002). Alternatively, they could "shift" posteriorly and reach the ventral branch of the tract through selective fasciculation. Finally, they could be removed through selective degeneration. To identify the mechanism involved, we observed the behavior of DN and VN axons as they elongate along the tract by confocal time-lapse imaging (Figure 2, Movies S1 and S2). We topographically injected dyes intraocularly at 48 hpf, began imaging at ∼54 hpf, and collected confocal z series every 15 min for up to 12 hr.

---

growth cones leading axons are intermingled. At 54 hpf (D and D′) and 60 hpf (E and E′), some DN axons are still missorted along VN axons (arrows). This missorting is no longer observed at 72 hpf (F and F′). Lateral views, confocal maximal projections; scale bar represents 20 µm. See also Figure S1. (G–I) Representative examples showing measurement of axon sorting in the tract at 48 hpf (G), 54 hpf (H), and 72 hpf (I). Intensity (Int, y axis) of DiD (blue) and DiI (red) signals was measured along a reference line drawn perpendicular to the tract (as indicated in C′). DiD signals are observed anteriorly to DiI signals at 48 and 54 hpf (arrows), but not at 72 hpf. (J) Quantification of missorting: a missorting index (MI) was calculated as the ratio of the signal intensity corresponding to missorted DN axons (D_R) to the signal intensity of all DN axons ($D_L + D_R$). DN axons were considered missorted when located anterior to the VN axons with the highest signal intensity. Missorting of DN axons is evident at 48 hpf and becomes progressively corrected by 72 hpf. Error bars correspond to SEs. **p < 0.05, ***p < 0.001.

Figure 1. Sorting of Retinal Axons in the Optic Tract Is Achieved through a Correction Mechanism

(A) DiD (blue) and DiI (red) were topographically injected into the DN and VN quadrants of the retina, respectively. Lateral view, confocal maximal projection. (B) Diagram of corresponding DN (blue) and VN (red) retinal projections observed at 72 hpf in a lateral view after removing the contralateral eye. The optic tract region is demarcated with orange dashed line. (C–F′) Dorsal axon trajectories are progressively corrected between 48 and 72 hpf. At 48 hpf, DN (C, blue in C′) and VN (red in C′) axons are not precisely sorted in the optic tract. Some DN axons (arrows) are observed along VN axons in the most anterior/dorsal part of the tract. DN (yellow arrowheads in C′) and VN (white arrowhead)
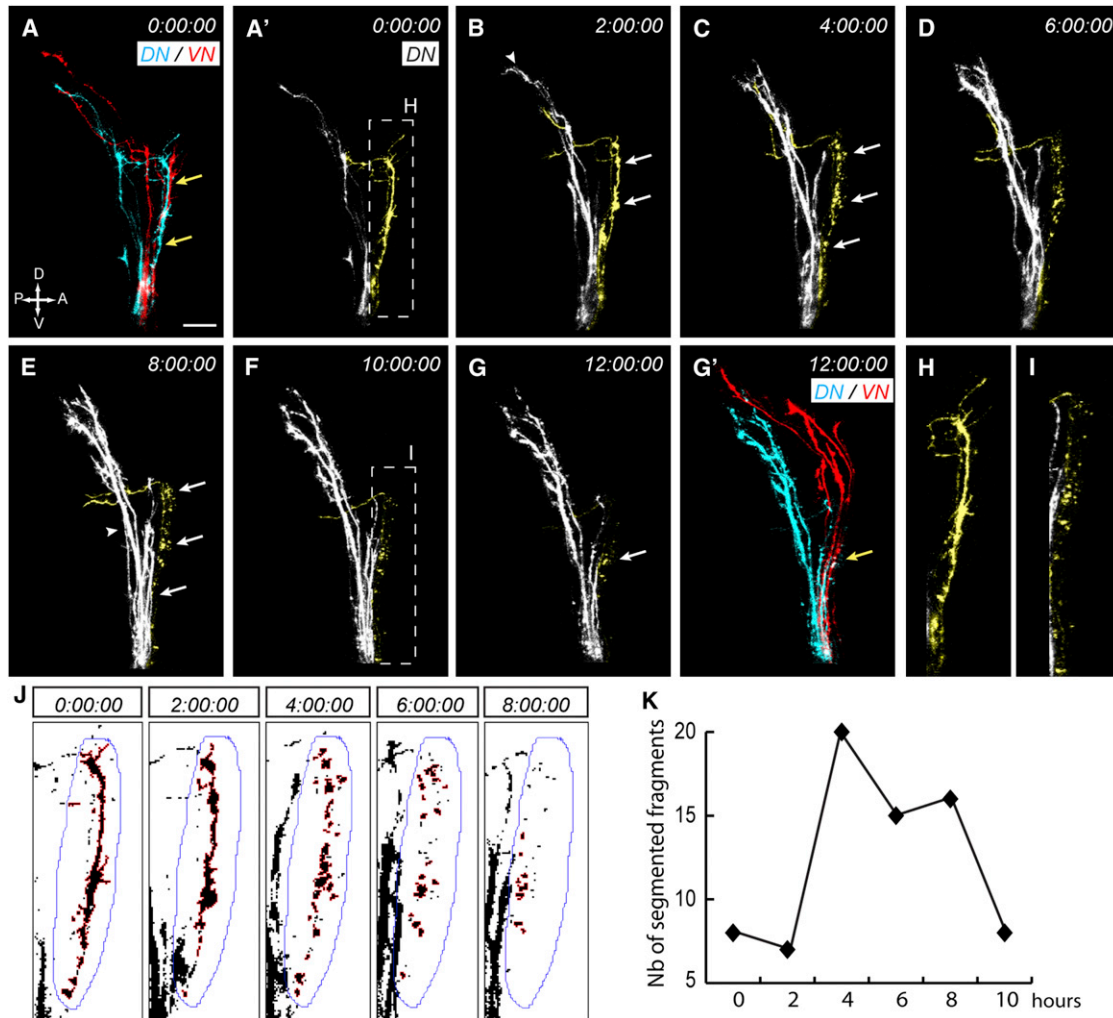
Figure 2. Missorted Dorsal Axons Selectively Degenerate

(A–G′) DN (blue, DiD) and VN (red, DiO) axons were topographically labeled at 48 hpf and time-lapse imaged at 15 min intervals for 12 hr starting at 54 hpf. The organization of DN and VN axons is shown at the beginning (A) and the end (G′) of the time-lapse, while time series of confocal image stack projections (A′–G) show DN axons only. Missorted DN axons are pseudocolored in yellow for the best visualization. Times indicate hours. Some DN axons are clearly missorted at 54 hpf (A′) and have a normal morphology (H). After 2 hr (B), correctly sorted axons have reached the tectum (arrowhead), while missorted DN axons stop their growth and start blebbing (arrows). They then fragment uniformly along their length over time (C–G, arrows), while correctly sorted axons (arrowhead in E) continue to grow toward the tectum. Fragments appear smaller at later stages (F, zoomed picture in I) and become hard to detect after 12 hr (G). Scale bar represents 20 μm. (See also Movies S1 and S2). (J) Maximal intensity projections of DiD signals at 0, 2, 4, 6, 8, and 10 hr (data not shown) were converted to binary images and a region of interest (ROI, blue line) surrounding missorted DN axons was defined. Axon segments within this region were then selected and analyzed using the "Analyze Particles" option in ImageJ. (K) Quantification of the number of axon fragments over time. Between 0 and 2 hr, the number of fragments is low, indicating that missorted axons are segmented as one main continuous region. The number of fragments then increases abruptly between 2 and 4 hr as axons degenerate and fragment. It then gradually decreases between 4 and 10 hr as axon fragments are progressively cleared. See also Figures S2 and S3.

Based on axon morphology and behavior, no evidence of photo-toxicity was observed. We also injected different combinations of dyes in various conditions to ensure that the dyes we used did not have any toxic effect (data not shown). In all our time-lapse analyses (n = 12), axons were very dynamic, elongating rapidly and sometimes pausing during their navigation. During these pauses, growth cones of correctly sorted axons harbored many dynamic filopodia that extended and retracted quickly. Interestingly, missorted DN axons had a different behavior. Although initially as dynamic as axons that were correctly sorted, they then stopped their elongation and became more quiescent. As they stopped, blebbing started to appear uniformly along their length (Figure 2B). This blebbing phase was rapidly followed by an abrupt and uniform fragmentation (Figures 2C–2F). Axonal fragments were of different sizes and appeared disconnected. Fragmentation of missorted DN axons was a rapid process, occurring over a period of 30 min (Movie S2, Figures 2J and 2K). Fragments became smaller over time and eventually disappeared (Figure 2G). This last clearance phase was slow and not always observed in our time-lapse conditions, even after

14 hr of imaging. Our observations thus indicate that topographic sorting of retinal axons along the optic tract is achieved through the selective degeneration of missorted DN axons. Interestingly, missorted DN axons always degenerated before reaching the tectum (n = 8), suggesting that degeneration is locally regulated.

The Degeneration of Missorted Axons Does Not Require Activation of Apoptotic Pathways or Neuronal Activity in RGCs

Axon degeneration is thought in other systems to rely on mechanisms distinct from cell body apoptosis (Nikolaev et al., 2009; Whitmore et al., 2003; Yan et al., 2010). To test whether activation of apoptotic pathways was required for correcting missorted DN axons, we analyzed axon sorting in the optic tract of *p53* morphants (Figure S2). No missorted DN axons were observed at 72 hpf when p53 was inhibited (MI 0.8%), indicating that correction occurred normally. Similarly, we did not observed any missorting defects after inhibiting caspase-3 or Bax activity (data not shown). These results suggest that specific signaling pathways distinct from apoptotic cascades or acting in parallel are involved in topographic sorting error correction.

We next examined whether neuronal activity in RGCs was required for optic tract sorting by analyzing retinal projections in *macho* (*mao*) mutants (Figure S3). The *mao* mutant was originally isolated in a screen for motility (Granato et al., 1996) and is characterized by a lack of voltage-gated Na+ current in RGCs and other neuronal types. As previously reported (Gnuegge et al., 2001; Trowe et al., 1996), we did not observe any sorting defects in *mao* (MI 0.9%), indicating that neuronal activity is not required for correcting missorted DN axons along the optic tract.

Heparan Sulfate Is Required for Topographic Sorting Error Correction

To identify which molecular mechanisms might regulate the degeneration of missorted DN axons, we decided to examine optic tract sorting in *dackel* (*dak*) mutants (Trowe et al., 1996). Our previous studies indicated that some DN axons are missorted at 60 hpf and 5 days postfertilization (dpf) in *dak* as a result of impaired heparan sulfate (HS) synthesis (Lee et al., 2004). However, it was not clear whether this was due to failure of correcting missorted DN axons at earlier stages. We found that sorting of retinal axons in *dak* mutants at 48 hpf was similar to that observed in wild-type (WT) embryos (Figures 3A and 3A'). Some DN axons elongated along or dorsally to VN axons in the most dorsal part of the tract, and growth cones leading axons were intermingled. As in WT embryos, missorted DN axons were still visible at 54 hpf, elongating along or dorsally to the dorsal branch of the tract (data not shown). However, in contrast to WT embryos, missorted axons were not corrected in *dak* mutants by 72 hpf (Figures 3B and 3B'). MIs were comparable at 48, 54, and 72 hpf (Figure 3E), indicating that the mechanism for correcting missorted DN axons is impaired in *dak* mutants.

If the correction mechanism required for sorting of retinal axons is deficient in *dak*, we predicted that restoring HS synthesis after axons have grown along the tract should rescue the phenotype. To test this hypothesis, we generated a rescue transgenic line heterozygous for the *dak* mutation and expressing the WT *ext2* gene (mutated in *dak*) under the control of a heat shock (*hsp70l*)-inducible promoter. We crossed this line to *dak* heterozygotes, performed heat shocks at different developmental times, and quantified the proportion of *dak* mutant embryos with missorted DN axons (Figure 3H). As expected, heat shocks performed before or during axon elongation along the tract (between 30 and 48 hpf) fully rescued the phenotype (Figures 3F and 3G), indicating that restoring Ext2 activity at early times is sufficient to produce HS that rescues sorting at later stages. Interestingly, heat shocks performed after axons had grown along the tract, from 48 to 69 hpf, also rescued missorting defects in *dak*. Rescue was no longer observed when heat shocks were performed after 72 hpf. This later period coincides with the onset of visually evoked responses from tectal neurons (Niell and Smith, 2005), suggesting that missorted axons might be stabilized by connections with synaptic partners. Thus, restoring HS synthesis at late stages in *dak* is sufficient to restore pretarget topographic sorting, indicating that the correction mechanism editing missorted axons along the tract requires the presence of HS.

Heparan Sulfate Acts Non-Cell-Autonomously to Correct Missorted Axons

HS is carried by diverse core proteins present at the cell surface or in the extracellular matrix. It could therefore act non-cell-autonomously in the environment and/or cell-autonomously at the surface of missorted DN axons. To determine where HS is required to correct missorted DN axons, we performed topographic transplantations of DN RGCs between WT and *dak* embryos carrying the *isl2b:EGFP* or *isl2b:TagRFP* transgenes, which are expressed in RGCs (Pittman et al., 2008) (Figure 4A). DN donor RGCs were transplanted between 30 and 34 hpf into the DN quadrant of the host retina, and their axonal projections were analyzed at 4 dpf. As in WT > WT transplants, *dak* RGCs transplanted into a WT host projected axons that were correctly sorted into the ventral branch of the tract (Figures 4C, 4C', 4E, and 4E'). In contrast, some axons of WT RGCs transplanted into a *dak* host were clearly missorted and elongated along the dorsal branch of the tract, as observed in *dak* > *dak* transplants (Figures 4B, 4B', 4D, and 4D'). Thus, HS is required non-cell-autonomously for correcting missorted DN axons and establishing pretarget topographic sorting.

DISCUSSION

Pretarget axon sorting is an important process contributing to the formation of topographic maps, yet the cellular and molecular mechanisms ordering axonal projections remain largely unknown. In this Report, we took advantage of the unique accessibility of the zebrafish embryo to determine how retinal axons are sorted along the dorsoventral axis in the optic tract before reaching the tectum. We showed that topographic sorting of retinal axons is not precisely established during initial growth cone pathfinding along the tract but is rather achieved through the selective degeneration of missorted axons. We further demonstrated that this specific developmental degeneration is regulated non-cell-autonomously by HS.
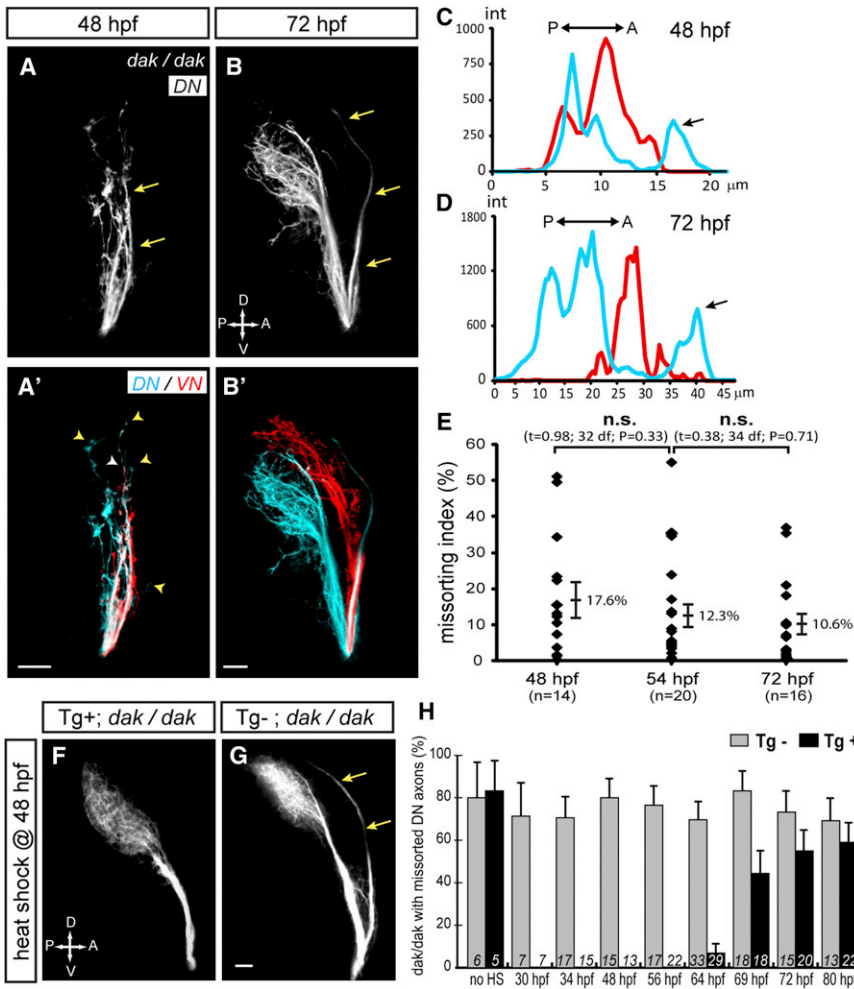
Figure 3. HS Is Required for Correcting Missorted DN Axons in the Tract

(A–B') DN (A and B, blue in A' and B') and VN (red in A' and B') retinal axons were topographically labeled at 48 and 72 hpf in *dak* mutants lacking HS. As observed in WT (Figure 1), some missorted DN axons are observed along VN axons at 48 hpf (arrows). DN (yellow arrowheads) and VN (white arrowhead) growth cones navigate along mixed trajectories (A'). In contrast to WT, however, missorted DN axons remain clearly visible at 72 hpf (arrows). Lateral views, confocal maximal projections; scale bar represents 20 μm. (C and D) Measurement of DiD and DiI signal intensities across the tract shows that missorted DN axons remain from 48 to 72 hpf in *dak*. (E) Missorting index (MI) is similar at 48, 54, and 72 hpf in *dak*, showing that missorted DN axons are not corrected. Error bars correspond to SEs. (F–H) Restoring HS synthesis at late stages in *dak* mutants corrects missorted DN axons. (F and G) *Tg(hsp70l:ext2-2A-TagRFP); dak* mutant embryos were heat shocked at 39°C for 1 hr at 48 hpf, fixed at 4 dpf, and their DN axons were topographically labeled with DiO. *dak* mutants carrying the rescue *ext2* transgene (Tg+, F) do not show any missorted DN axons, whereas *dak* sibling mutants lacking the transgene (Tg−, G) do (arrows). Lateral views, confocal maximal projections; scale bar represents 20 μm. (H) The proportion of *dak* mutants with missorted DN axons was scored at 4 dpf after embryos were heat shocked at various stages. In absence of heat shock, around 80% of *dak* mutants exhibit missorted DN axons. Heat shocks as late as 64 hpf correct missorting of DN axons in Tg+ but not in Tg− *dak* mutants. Error bars correspond to SEs.

The selective elimination of axons or dendrites is an essential process refining neuronal connections during development and establishing precise wiring of the nervous system. While programmed cell death has long been recognized as an important strategy for removing exuberant projections, it has become apparent that other mechanisms also remodel connections by locally eliminating inappropriate or misguided axons. Selective retraction of axon collaterals has been described in many systems as a pruning strategy to generate accurate patterns of connectivity. More recently, selective degeneration has emerged as another pruning mechanism for eliminating specific axons during development. It has mostly been described in *Drosophila*, where axons of the γ neurons in the mushroom bodies undergo fragmentation and locally degenerate during metamorphosis (Watts et al., 2003). In vertebrates, there are a limited number of studies suggesting that selective degeneration is used for eliminating inappropriate axon branches during the development of layer 5 subcortical projections and the retinotopic map after brain target has been reached (Luo and O'Leary, 2005). The contribution of selective axon degeneration to other developmental processes remains largely unknown, mostly because of the limited experimental approaches avail-

able in vivo in mammals. Using the zebrafish embryo as a model, we discovered a function for developmental degeneration in establishing precise pretarget topographic ordering of axons along a tract. Missorted retinal projections are selectively eliminated, leading to accurate and precise organization of axon fibers along the tract before they reach their brain target.

Observing the behavior of DN and VN axons directly in vivo as they elongate along the tract allowed us to show that pretarget topographic sorting of retinal axons is not precisely established during initial pathfinding. Growth cones are not precisely segregated according to their dorsoventral identity, and some DN axons elongate along with VN axons in the most dorsal part of the tract. Interestingly, only DN axons appear missorted, perhaps because VN axons act as pioneers and elongate along the tract first (Burrill and Easter, 1995). Missorted axons are initially very dynamic but eventually stop their elongation before reaching the tectum and rapidly fragment and degenerate. Axons always seem to pause before degenerating, suggesting that they might encounter a "stop" signal possibly leading to their degeneration. Whether stopping and degeneration are triggered coincidently by the same signal or independently by different cues remains to be determined. Blebbing and
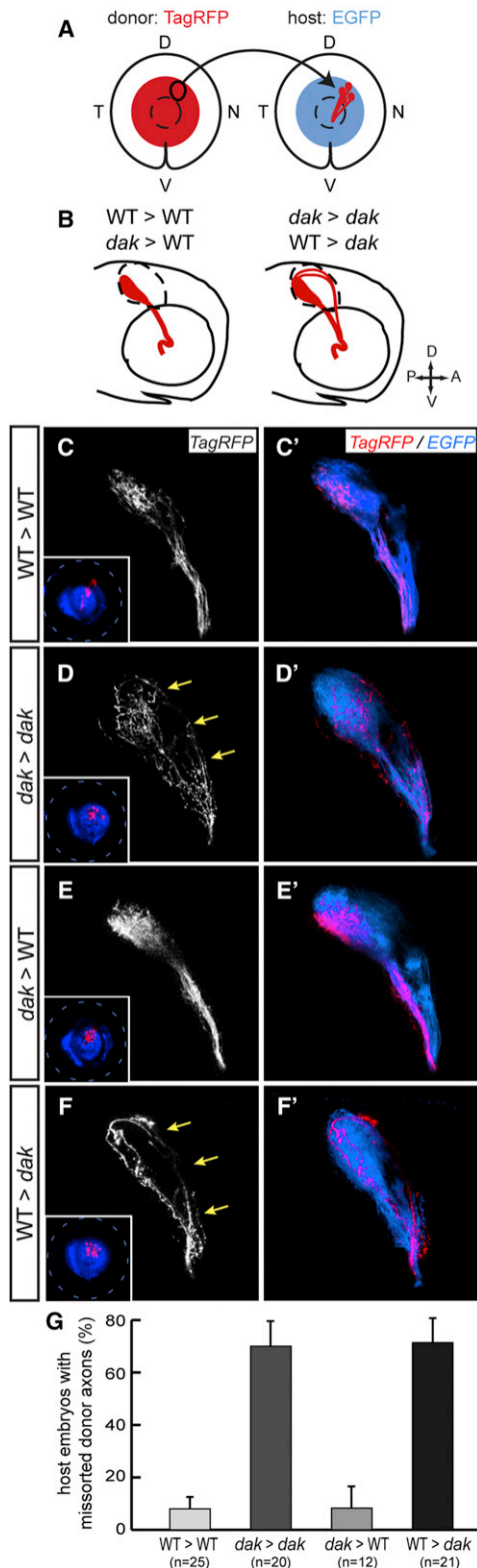
Figure 4. HS Is Required Non-Cell-Autonomously for Correct Sorting of DN Axons

(A) DN RGCs from an *isl2b:TagRFP* donor embryo were topographically transplanted between 30 and 34 hpf into the DN retina of an *isl2b:EGFP* host embryo. EGFP is shown in blue in the figure for the best visualization. (B–F′) Diagrams (B) and pictures (C–F′) of corresponding DN donor axons observed at 4 dpf. Lateral views, confocal maximal projections. In WT > WT (C and C′) and *dak* > WT (E and E′) transplants, DN donor axons (TagRFP+) pass through the ventral branch of the optic tract. In contrast, in *dak* > *dak* (D and D′) and WT > *dak* (F and F′) transplants, some donor axons are missorted along the dorsal branch of the tract (arrows) before reaching the tectum. Insets show transplanted DN TagRFP+ RGCs localized in the DN part of the host retina. (G) Quantification of missorting in transplants. The proportion of hosts with missorted donor DN axons was scored at 4 dpf. Missorting is observed in *dak* mutants but not WT hosts, indicating that HS is required non-cell-autonomously for correct sorting of retinal axons. Error bars correspond to SEs.

fragmentation are uniform along axonal length, indicating that degeneration is not initiated at the growth cone by a signal derived from the target but is rather locally regulated along the tract by spatially restricted cues. Interestingly, rotating the presumptive optic tract induces a corresponding turning of retinal axons (Harris, 1989), suggesting that axons react to local positional information on the neuroepithelium that might trigger their degeneration. That this information is independent from the brain target is further supported by the absence of sorting defects along the tract after ablation of the tectal primordia in frog (Reh et al., 1983).

As has been described in other developmental processes involving axon degeneration (Nikolaev et al., 2009; Whitmore et al., 2003; Yan et al., 2010), inhibiting p53, Bax, or caspase-3 activity did not prevent the selective degeneration of missorted DN axons, indicating that mechanisms distinct from cell body apoptosis or acting in parallel of apoptotic cascades are involved in topographic sorting error correction. Another parameter known to regulate developmental axon degeneration in some systems is neuronal activity. For instance, intrinsic neuronal activity is required for the selective elimination of callosal or subcortical axons (Luo and O'Leary, 2005). Similarly, retinal waves of activity are necessary for axon elimination leading to topographic map refinement in the superior colliculus in mammals (McLaughlin et al., 2003). In contrast, pretarget topographic sorting of retinal axons is normal in *mao* mutants that lack neuronal activity in RGCs. A possible explanation for this result is that correction of missorted axons occurs at early stages of development, before sensory stimulation or activity competition between axons might play a role.

We identified HS as a key regulator for correcting pretarget topographic sorting errors along the optic tract. While the importance of HS in axon guidance has been well described (Bülow et al., 2008; Lee and Chien, 2004), this is the first description, to our knowledge, of its role in modulating selective developmental degeneration. Interestingly, missorted DN axons pause and degenerate in WT but continue growing to the tectum in *dak*, suggesting that HS might also regulate a "stop" signal acting in parallel or prior to axonal degeneration.

HS is present at the cell surface or in the extracellular matrix as the glycosaminoglycan part of heparan sulfate proteoglycans (HSPGs). Interestingly, it is required non-cell-autonomously for correcting DN axons, suggesting different models for its mode of action. First, HS might function in the neuroepithelium as the specific cue triggering the degeneration of DN axons. HS could

then be carried by a core protein specifically expressed along the dorsal pathway or have specific structural motifs provided by HS-modifying enzymes that are themselves expressed preferentially at that location. Whether specific enzymes or core proteins are expressed in such distinctive patterns remains actually unknown. Alternatively, HS could act indirectly in the neuroepithelium by regulating the secretion or diffusion of a signaling molecule such as a guidance cue or a morphogen. Such cue would then be present in higher concentration along the dorsal branch of the tract. Finally, HS might be present at the surface of ventral axons and signals to the missorted dorsal axons elongating alongside. Such "communication" between ventral and dorsal axons would involve the presence of specific receptors at the surface of dorsal axons.

Whether HSPGs act directly on missorted axons or indirectly by modulating a signaling pathway remains to be determined. Interestingly, factors regulating map topography along the dorsoventral axis in the tectum such as Ephrin-Bs or Semaphorin-D (Hindges et al., 2002; Liu et al., 2004; Mann et al., 2002) do not seem to be involved in ordering axonal projections along the optic tract (Liu et al., 2004; Plas et al., 2008). These observations further suggest that the selective degeneration of missorted axons is locally regulated by an independent, specific pathway involving HSPGs. Syndecans and Glypicans are highly expressed in the nervous system and are known to modulate the signaling of guidance cues like Slits (Johnson et al., 2004; Rhiner et al., 2005; Steigemann et al., 2004) or of morphogens such as Wnt (Han et al., 2005; Muñoz et al., 2006). While Slit/Robo2 signaling does not seem to regulate sorting along the optic tract (data not shown), the Wnt pathway appears as an interesting candidate, as it has been shown to modulate developmental axon pruning in *C. elegans* and maintain axon stability in the olfactory system in the adult fly (Chiang et al., 2009; Hayashi et al., 2009). Determining whether specific Syndecans or Glypicans regulate similar pathways will be essential for a better understanding of axon tract formation and the etiology of related neurological disorders.

EXPERIMENTAL PROCEDURES

Detailed experimental procedures are available in the Supplemental Experimental Procedures.

Zebrafish
A detailed description of the strains used and manipulations of embryos are available in the Supplemental Experimental Procedures.

Visualization of Optic Tract Sorting in Fixed Embryos
RGCs in embryos fixed at 4 dpf were anterogradely labeled with the lipophilic dyes DiI or DiO (Molecular Probes, Invitrogen) using a vibrating needle injector (Baier et al., 1996). RGCs in embryos fixed at earlier stages were labeled with DiD and DiI using a dye-coated glass microneedle (Poulain et al., 2010). The contralateral eye was removed for imaging lateral views.

Quantification of Optic Tract Sorting
Confocal images of the optic tract were acquired with constant PMT voltage and gain throughout the z series. Stack images were imported in ImageJ and sum projected. Intensities of DiD (DN axons) and DiI (VN axons) signals were plotted along a reference line drawn perpendicular to the tract, 50 μm from the point where axons turn caudally to the tectum. A missorting index

(MI) was calculated as a ratio of signal intensities: (missorted DN axons)/(total DN axons). Statistical comparisons of MI used two-tailed Student's t tests.

Time-Lapse Imaging of Live Embryos
Embryos were anesthetized at 24 and 32 hpf to remove about half of the yolk and their left eye and at 48 hpf to perform topographic injection of DiD and DiO into the retina. Embryos were then mounted laterally at 54 hpf for time-lapse imaging. Z series were acquired at 15 min intervals for up to 14 hr. Maximal intensity projections for each time point were compiled, pseudocolored, and aligned using ImageJ software and StackReg plugin.

Quantification of Missorted DN Axon Fragmentation
For each time-lapse, maximal intensity projections of DiD signals at 0, 2, 4, 6, 8, and 10 hr were converted to binary images. A region of interest (ROI) was defined at t = 0 along the dorsal branch of the optic tract as an ellipse surrounding missorted dorsal axons. The number of axonal segments within the ROI was quantified over time using the "Analyze Particles" option in ImageJ. A threshold of 4pixel^2 was used to eliminate background signal.

Heat Shock
Embryos were left at room temperature for 30 min and then transferred at 39°C for 1 hr at different developmental times. They were fixed at 4 dpf, and dorsal retinal projections were labeled by injection of DiO. The proportion of $dak-/-$ mutants with missorted DN axons was scored in three independent experiments for each time point embryos were heat shocked.

Topographic Transplantations
Topographic transplantations were performed as recently described in Poulain et al. (2010). Projections of donor axons were imaged at 4 dpf by live confocal microscopy.

SUPPLEMENTAL INFORMATION

Supplemental Information includes three figures, Supplemental Experimental Procedures, and two movies and can be found with this article online at http://dx.doi.org/10.1016/j.neuron.2013.02.005.

REFERENCES

Baier, H., Klostermann, S., Trowe, T., Karlstrom, R.O., Nüsslein-Volhard, C., and Bonhoeffer, F. (1996). Genetic dissection of the retinotectal projection. Development *123*, 415–425.

Bozza, T., Vassalli, A., Fuss, S., Zhang, J.J., Weiland, B., Pacifico, R., Feinstein, P., and Mombaerts, P. (2009). Mapping of class I and class II odorant receptors to glomerular domains by two distinct types of olfactory sensory neurons in the mouse. Neuron *61*, 220–233.

Bülow, H.E., Tjoe, N., Townley, R.A., Didiano, D., van Kuppevelt, T.H., and Hobert, O. (2008). Extracellular sugar modifications provide instructive and cell-specific information for axon-guidance choices. Curr. Biol. *18*, 1978–1985.

Burrill, J.D., and Easter, S.S., Jr. (1995). The first retinal axons and their microenvironment in zebrafish: cryptic pioneers and the pretract. J. Neurosci. *15*, 2935–2947.

Chan, S.O., and Guillery, R.W. (1994). Changes in fiber order in the optic nerve and tract of rat embryos. J. Comp. Neurol. *344*, 20–32.

Chiang, A., Priya, R., Ramaswami, M., Vijayraghavan, K., and Rodrigues, V. (2009). Neuronal activity and Wnt signaling act through Gsk3-beta to regulate axonal integrity in mature Drosophila olfactory sensory neurons. Development *136*, 1273–1282.

Feldheim, D.A., and O'Leary, D.D. (2010). Visual map development: bidirectional signaling, bifunctional guidance molecules, and competition. Cold Spring Harb. Perspect. Biol. *2*, a001768.

Gnuegge, L., Schmid, S., and Neuhauss, S.C. (2001). Analysis of the activity-deprived zebrafish mutant macho reveals an essential requirement of neuronal activity for the development of a fine-grained visuotopic map. J. Neurosci. *21*, 3542–3548.

Granato, M., van Eeden, F.J., Schach, U., Trowe, T., Brand, M., Furutani-Seiki, M., Haffter, P., Hammerschmidt, M., Heisenberg, C.P., Jiang, Y.J., et al. (1996). Genes controlling and mediating locomotion behavior of the zebrafish embryo and larva. Development *123*, 399–413.

Han, C., Yan, D., Belenkaya, T.Y., and Lin, X. (2005). Drosophila glypicans Dally and Dally-like shape the extracellular Wingless morphogen gradient in the wing disc. Development *132*, 667–679.

Harris, W.A. (1989). Local positional cues in the neuroepithelium guide retinal axons in embryonic Xenopus brain. Nature *339*, 218–221.

Hayashi, Y., Hirotsu, T., Iwata, R., Kage-Nakadai, E., Kunitomo, H., Ishihara, T., Iino, Y., and Kubo, T. (2009). A trophic role for Wnt-Ror kinase signaling during developmental pruning in Caenorhabditis elegans. Nat. Neurosci. *12*, 981–987.

Hindges, R., McLaughlin, T., Genoud, N., Henkemeyer, M., and O'Leary, D.D. (2002). EphB forward signaling controls directional branch extension and arborization required for dorsal-ventral retinotopic mapping. Neuron *35*, 475–487.

Hutson, L.D., and Chien, C.B. (2002). Pathfinding and error correction by retinal axons: the role of astray/robo2. Neuron *33*, 205–217.

Imai, T., Yamazaki, T., Kobayakawa, R., Kobayakawa, K., Abe, T., Suzuki, M., and Sakano, H. (2009). Pre-target axon sorting establishes the neural map topography. Science *325*, 585–590.

Johnson, K.G., Ghose, A., Epstein, E., Lincecum, J., O'Connor, M.B., and Van Vactor, D. (2004). Axonal heparan sulfate proteoglycans regulate the distribution and efficiency of the repellent slit during midline axon guidance. Curr. Biol. *14*, 499–504.

Lee, J.S., and Chien, C.B. (2004). When sugars guide axons: insights from heparan sulphate proteoglycan mutants. Nat. Rev. Genet. *5*, 923–935.

Lee, J.S., von der Hardt, S., Rusch, M.A., Stringer, S.E., Stickney, H.L., Talbot, W.S., Geisler, R., Nüsslein-Volhard, C., Selleck, S.B., Chien, C.B., and Roehl, H. (2004). Axon sorting in the optic tract requires HSPG synthesis by ext2 (dackel) and extl3 (boxer). Neuron *44*, 947–960.

Liu, Y., Berndt, J., Su, F., Tawarayama, H., Shoji, W., Kuwada, J.Y., and Halloran, M.C. (2004). Semaphorin3D guides retinal axons along the dorsoventral axis of the tectum. J. Neurosci. *24*, 310–318.

Luo, L., and O'Leary, D.D. (2005). Axon retraction and degeneration in development and disease. Annu. Rev. Neurosci. *28*, 127–156.

Mann, F., Ray, S., Harris, W., and Holt, C. (2002). Topographic mapping in dorsoventral axis of the Xenopus retinotectal system depends on signaling through ephrin-B ligands. Neuron *35*, 461–473.

McLaughlin, T., Torborg, C.L., Feller, M.B., and O'Leary, D.D. (2003). Retinotopic map refinement requires spontaneous retinal waves during a brief critical period of development. Neuron *40*, 1147–1160.

Muñoz, R., Moreno, M., Oliva, C., Orbenes, C., and Larraín, J. (2006). Syndecan-4 regulates non-canonical Wnt signalling and is essential for convergent and extension movements in Xenopus embryos. Nat. Cell Biol. *8*, 492–500.

Niell, C.M., and Smith, S.J. (2005). Functional imaging reveals rapid development of visual response properties in the zebrafish tectum. Neuron *45*, 941–951.

Nikolaev, A., McLaughlin, T., O'Leary, D.D., and Tessier-Lavigne, M. (2009). APP binds DR6 to trigger axon pruning and neuron death via distinct caspases. Nature *457*, 981–989.

Pittman, A.J., Law, M.Y., and Chien, C.B. (2008). Pathfinding in a large vertebrate axon tract: isotypic interactions guide retinotectal axons at multiple choice points. Development *135*, 2865–2871.

Plas, D.T., Lopez, J.E., and Crair, M.C. (2005). Pretarget sorting of retinocollicular axons in the mouse. J. Comp. Neurol. *491*, 305–319.

Plas, D.T., Dhande, O.S., Lopez, J.E., Murali, D., Thaller, C., Henkemeyer, M., Furuta, Y., Overbeek, P., and Crair, M.C. (2008). Bone morphogenetic proteins, eye patterning, and retinocollicular map formation in the mouse. J. Neurosci. *28*, 7057–7067.

Poulain, F.E., Gaynes, J.A., Stacher Hörndli, C., Law, M.Y., and Chien, C.B. (2010). Analyzing retinal axon guidance in zebrafish. Methods Cell Biol. *100*, 3–26.

Reh, T.A., Pitts, E., and Constantine-Paton, M. (1983). The organization of the fibers in the optic nerve of normal and tectum-less Rana pipiens. J. Comp. Neurol. *218*, 282–296.

Rhiner, C., Gysi, S., Fröhli, E., Hengartner, M.O., and Hajnal, A. (2005). Syndecan regulates cell migration and axon guidance in C. elegans. Development *132*, 4621–4633.

Satoda, M., Takagi, S., Ohta, K., Hirata, T., and Fujisawa, H. (1995). Differential expression of two cell surface proteins, neuropilin and plexin, in Xenopus olfactory axon subclasses. J. Neurosci. *15*, 942–955.

Scholes, J.H. (1979). Nerve fibre topography in the retinal projection to the tectum. Nature *278*, 620–624.

St John, J.A., Clarris, H.J., McKeown, S., Royal, S., and Key, B. (2003). Sorting and convergence of primary olfactory axons are independent of the olfactory bulb. J. Comp. Neurol. *464*, 131–140.

Steigemann, P., Molitor, A., Fellert, S., Jäckle, H., and Vorbrüggen, G. (2004). Heparan sulfate proteoglycan syndecan promotes axonal and myotube guidance by slit/robo signaling. Curr. Biol. *14*, 225–230.

Stuermer, C.A. (1988). Retinotopic organization of the developing retinotectal projection in the zebrafish embryo. J. Neurosci. *8*, 4513–4530.

Trowe, T., Klostermann, S., Baier, H., Granato, M., Crawford, A.D., Grunewald, B., Hoffmann, H., Karlstrom, R.O., Meyer, S.U., Müller, B., et al. (1996). Mutations disrupting the ordering and topographic mapping of axons in the retinotectal projection of the zebrafish, Danio rerio. Development *123*, 439–450.

Watts, R.J., Hoopfer, E.D., and Luo, L. (2003). Axon pruning during Drosophila metamorphosis: evidence for local degeneration and requirement of the ubiquitin-proteasome system. Neuron *38*, 871–875.

Whitmore, A.V., Lindsten, T., Raff, M.C., and Thompson, C.B. (2003). The proapoptotic proteins Bax and Bak are not involved in Wallerian degeneration. Cell Death Differ. *10*, 260–261.

Yan, T., Feng, Y., and Zhai, Q. (2010). Axon degeneration: Mechanisms and implications of a distinct program from cell death. Neurochem. Int. *56*, 529–534.